The American Journal of Pathology, Vol. 177, No. 1, July 2010

DOI: 10.2353/ajpath.2010.090592

Musculoskeletal Pathology

Bisphosphonates Cause Osteonecrosis of the Jaw-Like Disease in Mice

Yanming Bi,* Yamei Gao,† Driss Ehirchiou,† Chunzhang Cao,† Takashi Kikuiri,‡ Anh Le,‡ Songtao Shi,‡ and Li Zhang†

From the Craniofacial and Skeletal Diseases Branch, National Institute of Dental and Craniofacial Research, National Institutes of Health, Bethesda, Maryland; the Center for Vascular and Inflammatory Diseases,† the Department of Physiology, University of Maryland School of Medicine, Baltimore, Maryland; and the Center for Craniofacial Molecular Biology,‡ University of Southern California School of Dentistry, Los Angeles, California*

Bisphosphonate-associated osteonecrosis of the jaw (BONJ) is a morbid bone disease linked to long-term bisphosphonate use. Despite its broad health impact, mechanistic study is lacking. In this study, we have established a mouse model of BONJ-like disease based on the equivalent clinical regimen in myeloma patients, a group associated with high risk of BONJ. We demonstrate that the murine BONJ-like disease recapitulates major clinical and radiographical manifestations of the human disease, including characteristic features of osseous sclerosis, sequestra, avascular, and radiopaque alveolar bone in the jaw that persists beyond a normal course of wound healing following tooth extraction. We find that long-term administration of bisphosphonates results in an increase in the size and number of osteoclasts and the formation of giant osteoclast-like cells within the alveolar bone. We show that the development of necrotic bone and impaired soft tissue healing in our mouse model is dependent on long-term use of high-dose bisphosphonates, immunosuppressive and chemotherapy drugs, as well as mechanical trauma. Most importantly, we demonstrate that bisphosphonate is the major cause of BONJ-like disease in mice, mediated in part by its ability to suppress osseous angiogenesis and bone remodeling. The availability of this novel mouse model of BONJ-like disease will help elucidate the pathophysiology of BONJ and ultimately develop novel approaches for prevention and treatment of human BONJ. ***(Am J Pathol 2010, 177:280–290; DOI: 10.2353/ajpath.2010.090592)***

Bisphosphonates represent a major class of antiresorptive drug to manage skeletal complications in patients suffering from Paget's disease, bone metastases of multiple myeloma, breast and prostate cancers, and osteoporosis.[1–5] Administration of bisphosphonates in these patients effectively restores bone mineral density and bone strength, reduces the incidence of bone fracture, and dramatically improves their quality of life. Despite these beneficial effects, a growing number of cancer patients on long-term and high-dose bisphosphonate therapy develop osteonecrosis of the jaw (BONJ),[1–4] a devastating disease characterized by osteocyte death within the alveolar jaw bone. BONJ is an urgent clinical problem, especially in cancer patients with bone metastases and specifically the multiple myeloma patients, and no effective treatment is available.[5]

The majority of BONJ cases have been reported in patients taking intravenous injections of zoledronate (Zometa), a nitrogen-containing bisphosphonate (aminobisphosphonate), with a small number cases associated with another aminobisphosphonate, pamidronate (Aredia).[1–4,6–8] Risk factors for BONJ include invasive dental procedures, infections, mechanical trauma to the jaw bone, and length of exposure to bisphosphonates, as well as concomitant use of immunosuppressive and chemotherapy drugs.[1–4,8] Patients with BONJ present various jaw symptoms, including pain, swelling, infection, loose teeth, and exposed bones in some severe cases.[1–4] Histologically, BONJ manifests in diverse tissue changes, including necrotic bone honeycombed with residual vital bone, inflammatory cellular elements, and fibrous tissues.[9] Standard osseous sequestrectomy usually results in enlarged bony defects.[2–4] Currently, only conservative non-surgical methods are recommended, which only slows down the deterioration but does not cure the disease.[5] Therefore, there is an urgent need to understand the etiology of BONJ, determine the risk factors, and develop an effective modality to prevent and treat BONJ in cancer patients.

Supported in part by the Division of Intramural Research, National Institute of Dental and Craniofacial Research, National Institutes of Health and NIH grants HL054710 and AI078365.

Accepted for publication March 1, 2010.

Address reprint requests to Li Zhang, Ph.D., University of Maryland School of Medicine, 800 W. Baltimore Street, Baltimore, MD 21201. E-mail: lizhang@som.umaryland.edu.

A major obstacle to our understanding of the pathophysiology of BONJ is the inability to conduct prospective well-controlled clinical studies, especially in the high-risk cancer patients that are taking multiple medications to control both tumor growth and its related skeletal complications. Thus, animal models of BONJ are urgently needed to decipher its underlying cause and to resolve the controversies regarding the role of bisphosphonates in the pathogenesis of this disease. In this work, we report the development of the first mouse model of BONJ-like disease. Most importantly, our results demonstrate that bisphosphonate is the major cause of BONJ.

Materials and Methods

Animals

Wild-type C57BL6 mice 8 to 12 weeks old, purchased from the National Cancer Institute (Frederick, MD), were used in all experiments. Animals were housed in a pathogen-free facility, and all procedures were performed in accordance with Institutional Animal Care and Use Committee approval.

Bisphosphonate-Induced Osteonecrosis of the Jaw

Mice were injected intraperitoneally with zoledronate (125 μg/kg body weight; twice per week), dexamethasone (Dex; 5 mg/kg body weight, weekly), docetaxel (25 mg/kg, weekly) or their combinations before tooth extraction for 3 weeks. The first molar tooth from either left maxillary (upper left jaw) or right mandible (lower right jaw) was extracted with a molar luxator. After extraction, the above different drugs or drug combinations were continuously injected for 3 to 12 weeks. Thereafter, mice were euthanized and perfused with saline and then with 2% periodate-lysine-paraformaldehyde solution (2% paraformaldehyde, 75 mmol/L lysine, and 10 mmol/L sodium periodate solution, pH 7.4). The right and left maxillary bones were retrieved, analyzed by microcomputed tomography (μCT) and then decalcified in EDTA-glycerol solution (14.5% EDTA and 15% glycerol) at 4°C for 2 to 3 weeks. Paraffin-embedded samples were sectioned (5 μm) and subjected to histochemical staining.

Histochemistry and Immunohistochemistry

Paraffin-embedded 5-μm-thick sections were analyzed histochemically by hematoxylin and eosin (H&E) staining, based on our published procedures.[10] Osteoclasts were identified by tartrate-resistant acidic phosphatase (TRAP) staining using a leukocyte acid phosphatase kit (Sigma, St. Louis, MO), following the procedures recommended by the manufacturer. Osteoblasts were identified by their positive alkaline phosphatase (ALP) staining as previously described[11] and the presence of mature osteoblasts was further confirmed by positive staining for matrix-associated osteocalcin using rabbit anti-mouse osteocalcin antibody (Lifespan Biosciences, Seattle, WA) following the manufacturer's instructions. Briefly, deparaffinized tissue slides were incubated with anti-mouse osteocalcin at 4°C overnight. Isotype-matched control antibodies (Zymed) were used under the same condition. The broad-spectrum immunoperoxidase AEC kit (Picture Plus, Zymed) was used to detect immunoreactivity, and hematoxylin was used for counter stain.

Quantification of Necrotic Bone

To quantify the degree of osteonecrosis, four uniformly spaced H&E-stained sections (#10, #20, #30, and #40) of the left maxillary jaw from each animal were scanned digitally using a ScanScope slide scanner (Aperio Technologies, Vista, CA). An area of interest (~0.9 mm^2) located within 1.2 mm of the number 2 molar was selected. The dead bone, defined as any 1000-μm^2 area that contains three or more empty lacunae, was marked. The total areas of dead bone were determined for each section using ImageScope. An average value of dead bone area was calculated over the above four sections per mouse. Bone histomorphometric analysis was performed according to the American Society for Bone and Mineral Research nomenclature guideline.[12] Briefly, osteoclasts were identified as TRAP$^+$ multinucleate cells. The number of osteoclasts and giant osteoclasts (those containing 10 or more nuclei) within the region of interests was counted. The length (in millimeters) of the alveolar bone surface covered by TRAP$^+$ multinucleate cells (osteoclast surface) and the length of total alveolar bone surface (bone surface) were measured using the ImageScope software. Statistical analysis was done using Student's *t*-test in the SigmaPlot software (Systat Software, Inc.). The group size ranged from 3 to 11 mice.

Bone Remodeling and Osseous Angiogenesis

For dynamic bone histomorphometric analysis, calcein (20 mg/kg body weight; Sigma) and alizarin complexone (35 mg/kg body weight; Sigma) were injected intraperitoneally into bisphosphonate- or vehicle-treated mice at 4 weeks and 6 weeks after extraction to label actively forming bone surfaces. For vascular labeling, mice were perfused before tissue collection with saline to remove blood cells and then with 0.5 mg/ml fluorescein isothiocyanate (FITC)-conjugated bovine serum albumin (BSA) in 2.5% gelatin to fill all functional vessels, based on the published method.[13] The maxillary bones were then retrieved and fixed in cold 2% periodate-lysine-paraformaldehyde overnight, embedded in optimum cutting temperature (OCT) compound (Tissue-Tek, Sakura), and cut into 10-μm frozen sections onto a Cryofilm (FINETEC Co. Ltd, Japan) using a Leica CM1900 cryostat (Leica, Inc., Nussloch, Germany). The presence of blood vessels was confirmed by positive staining of an endothelial cell marker CD31, using rat anti-CD31 antibody (BD/PharMingen, San Diego, CA) followed by Alexa Fluor 594 goat anti-rat IgG. Incorporation of calcein-derived green fluorescence and alizarin-derived red fluorescence in the

alveolar bone, as well as visualization of the FITC-filled blood vessels and CD31-positive capillaries, were conducted by fluorescent microscopy.

Microcomputed Tomography Analysis

Mouse maxillary bones were scanned and reconstructed with 8-μm isotropic voxels on a μCT system (eXplore MS, GE Medical Systems, London, Ontario, Canada). The two-dimensional and three-dimensional images of the maxilla were reconstructed using MicroView (GE Medical Systems).

Statistical Analysis

Representative figures of at least three independent experiments were shown. Statistical analyses were performed using Student's *t*-test (Systat Software, Inc., Point Richmond, CA). *P* values less than 0.05 were considered significant.

Results

Mechanic Injury Leads to Transient Osteocyte Loss within Alveolar Bone

Bisphosphonate-associated osteonecrosis primarily occurs in the jaw, particularly following dental procedures.[1–4] Mechanical injury of the jaw, either by dental surgery or caused by daily wear, could induce BONJ in patients on bisphosphonate therapy. To test the hypothesis that necrosis of the jaw bone was initiated by mechanical injury, we extracted the first molar of the left maxilla (Figure 1A, right panel). One day after tooth extraction, the empty alveolar socket was filled with amorphous thrombi (Figure 1B, asterisks). The osteocytes resided closely to the thrombus at the depth of the void extraction socket were lost, creating a narrow zone of dead bone with empty lacunae (Figure 1B, bottom panel, yellow dotted line).

Three days after the injury, numerous mesenchymal cells were recruited within the provisional matrix (Figure 1C, upper right panel), and new capillary-like structures have emerged (Figure 1C, bottom left panel, blue arrows). Necrotic bone, identified by the presence of empty lacunae (Figure 1C, bottom right panel, yellow arrows),

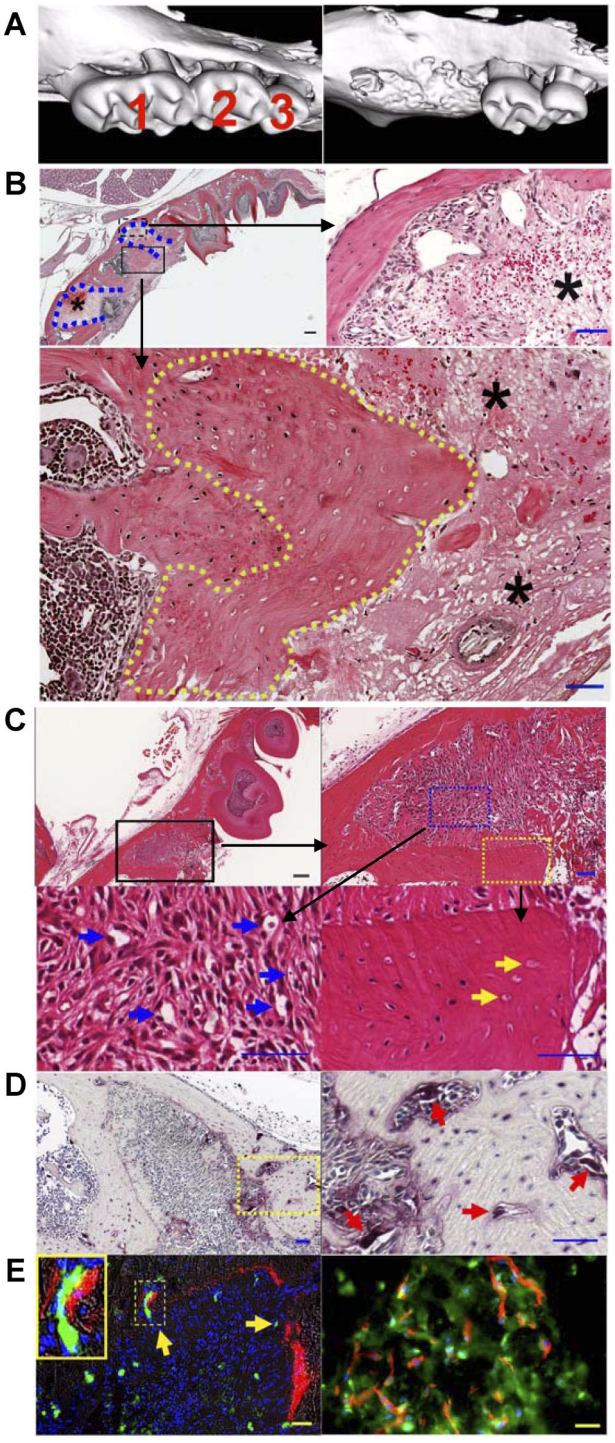

Figure 1. Tooth injury leads to the development of necrotic bone and promotes osseous angiogenesis and bone remodeling. **A:** Three-dimensional reconstruction of μCT images of the left maxilla from mice without (**left**) and with (**right**) tooth extraction. **B:** H&E staining of the paraffin-embedded sections of the left maxilla from mice at one day after tooth extraction of the first left maxillary molar (**top left**; Scale bar = 200 μm). **Blue dotted lines** indicate the extraction socket. Higher magnification image shows the presence of amorphous thrombi (**top right panel**; **asterisks**) within the extraction tooth sockets and the dead bone with empty lacunae (**bottom panel**; **yellow dotted line**), respectively. Scale bar = 50 μm. **C:** H&E staining of the left maxilla three days after tooth extraction. The **top panels** show the low (**left**; Scale bar = 200 μm) and high (**right**; Scale bar = 50 μm) magnification images of the extraction socket. The **bottom panels** show the presence of abundant mesenchymal cells and capillary-like structures (**left**; **blue arrows**) within the provisional matrix and the presence of necrotic bone with empty lacunae (**right**; **yellow arrows**) adjacent to the amorphous thrombi. Scale bars = 50 μm. **D:** TRAP staining. Three days after extraction, abundant $TRAP^+$ osteoclasts (purple) were found on the alveolar bone surface within the extraction socket (**left**; Scale bar = 200 μm). Higher magnification of the **yellow dotted area** was shown in the **right panel** (**red arrows** indicate osteoclasts; Scale bar = 50 μm). **E:** Bone and blood vessel formation. Alizarin complexone labeling on day one and FITC-BSA perfusion on day three following extraction reveal the formation of new bone (**left**; red fluorescence) and the presence of functional blood vessels (green fluorescence; **yellow arrows**). **Inset** shows newly formed bone adjacent to a blood vessel. Scale bar = 50 μm. Immunofluorescent staining in the **right panel** shows the presence of $osteocalcin^+$ bone matrix (green) residing proximally to $CD31^+$ capillaries (red). DAPI-stained nuclei are shown in blue. Scale bar = 20 μm.

remained adjacent to the amorphous thrombi. Bone remodeling may have been initiated, as numerous TRAP$^+$ osteoclasts were found on the bone surface (Figure 1D, right panel, red arrows).

To verify that the capillary-like structure within the provisional matrix (Figure 1C, bottom left panel, blue arrows) were indeed newly formed blood vessels, mice were injected intraperitoneally with alizarin complexone 1 day and perfused with FITC-BSA 3 days after injury. Immediately after perfusion, the left maxillary jaw bone was retrieved and frozen sections were prepared. Consistent with the above findings of new emerging capillary-like structures within the provisional matrix (Figure 1C, bottom left panel), we observed abundant FITC$^+$ blood vessels (green) in the same provisional matrix (Figure 1E, left panel, yellow arrows). Additionally, we found that newly formed bone tissue (red) resided closely to the capillaries (green) (Figure 1E, left panel, inset). Immunofluorescent staining using antibodies against CD31 (an endothelial cell marker; in red) and osteocalcin (a matrix protein produced by mature osteoblasts; in green) confirmed the presence of emerging blood vessels in the newly formed bone (Figure 1E, right panel). These results indicate that tooth extraction led to the initial death of the alveolar bone, which was repaired through increased osseous angiogenesis and bone remodeling.

Bisphosphonates Suppress Angiogenesis and Bone Remodeling in Osseous Tissues

To investigate whether administration of bisphosphonates would suppress angiogenesis and subsequently bone remodeling within the osseous tissues in response to injury, we treated mice (5 mice per group) with PBS (Figure 2, left panels) or zoledronate (Figure 2, right panels) for 7 days (no pretreatment). Bone remodeling was probed by injecting intraperitoneally with alizarin 2 days after tooth extraction. On day 7, mice were perfused with FITC-BSA to label the functional blood vessels. We observed new bone formation (in red) on the surface of the alveolar bone and also within the extraction socket, which was suppressed by injection of zoledronate (Figure 2A, right panel). In addition, we found that zoledronate strongly suppressed angiogenesis within the extraction sockets, resulting in fewer FITC$^+$ capillaries within the provisional matrix (Figure 2B, right panel, green fluorescence). Consistent with the lower bone remodeling activity in zoledronate-treated mice, we found that zoledronate injection reduced the number of both osteoclasts, based on TRAP staining (Figure 2C, right panel, red arrows) and osteoblasts, based on staining with an osteogenic cell marker ALP (Figure 2D, right panel, red) and a mature osteoblast marker osteocalcin (Figure 2E, right panel, brown) within the extraction sockets.

Bisphosphonate Treatment Leads to the Development of BONJ-Like Disease

The above results demonstrated that bisphosphonate injection in mice suppressed both angiogenesis and bone remodeling. Based on these observations, we hypothesized that dual suppression by bisphosphonates may lead to development of BONJ-like disease in mice. To test this hypothesis, we sought to develop a mouse model of BONJ-like disease by mimicking the clinical regimen in multiple myeloma patients, a group of cancer patients with high risk of BONJ. In particular, we aimed to replicate the following observations: i) BONJ patients are more likely on combination therapy including high dose of bisphosphonates and immunosuppressive drugs such as steroids or/and chemotherapeutic agents; ii) BONJ is

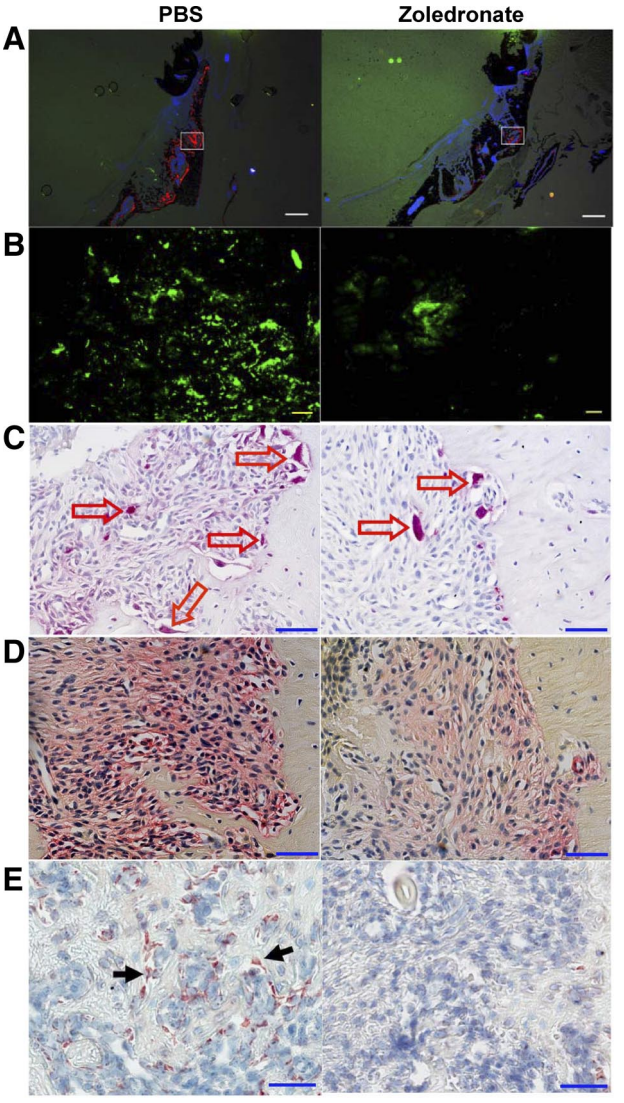

Figure 2. Bisphosphonates suppress angiogenesis and bone remodeling in osseous tissues in response to injury. Mice were treated with PBS (**left panels**) or zoledronate (**right panels**) for one week following tooth extraction (no pretreatment), and then injected with alizarin 4 days and perfused with FITC-BSA 7 days later. **A:** Fluorescent images of the frozen sections of the left maxilla showed alizarin incorporation for bone formation (red fluorescence). Scale bars = 500 μm. **B:** Higher magnification images of the **white squares in A** show the presence of osseous angiogenesis (green), which was suppressed by zoledronate treatment (**right**). Scale bars = 50 μm. **C:** TRAP staining of the paraffin-embedded sections of the left maxilla showed the presence of TRAP$^+$ osteoclasts (**red arrows**). **D:** ALP staining of the paraffin-embedded sections of the left maxilla showed the presence of osteoblasts and their precursor cells (red color). **E:** Immunohistochemistry shows the presence of osteocalcin$^+$ mature osteoblasts (**black arrows**). Scale bars for to **C–E:** 50 μm.

almost exclusively associated with nitrogen-containing bisphosphonates, eg, zoledronate and pamidronate; iii) clinical manifestations of BONJ are often reported in bisphosphonate-treated patients following some dental procedures or mucosal injury in the oral cavity; and iv) BONJ affects both maxilla and mandible.[1–5] Accordingly, we treated C57BL6 mice with zoledronate and dexamethasone. The selected dosage of zoledronate (125 μg/kg body weight; twice per week) is equivalent to the high concentration (4 mg; intravenously every 3 to 4 weeks)

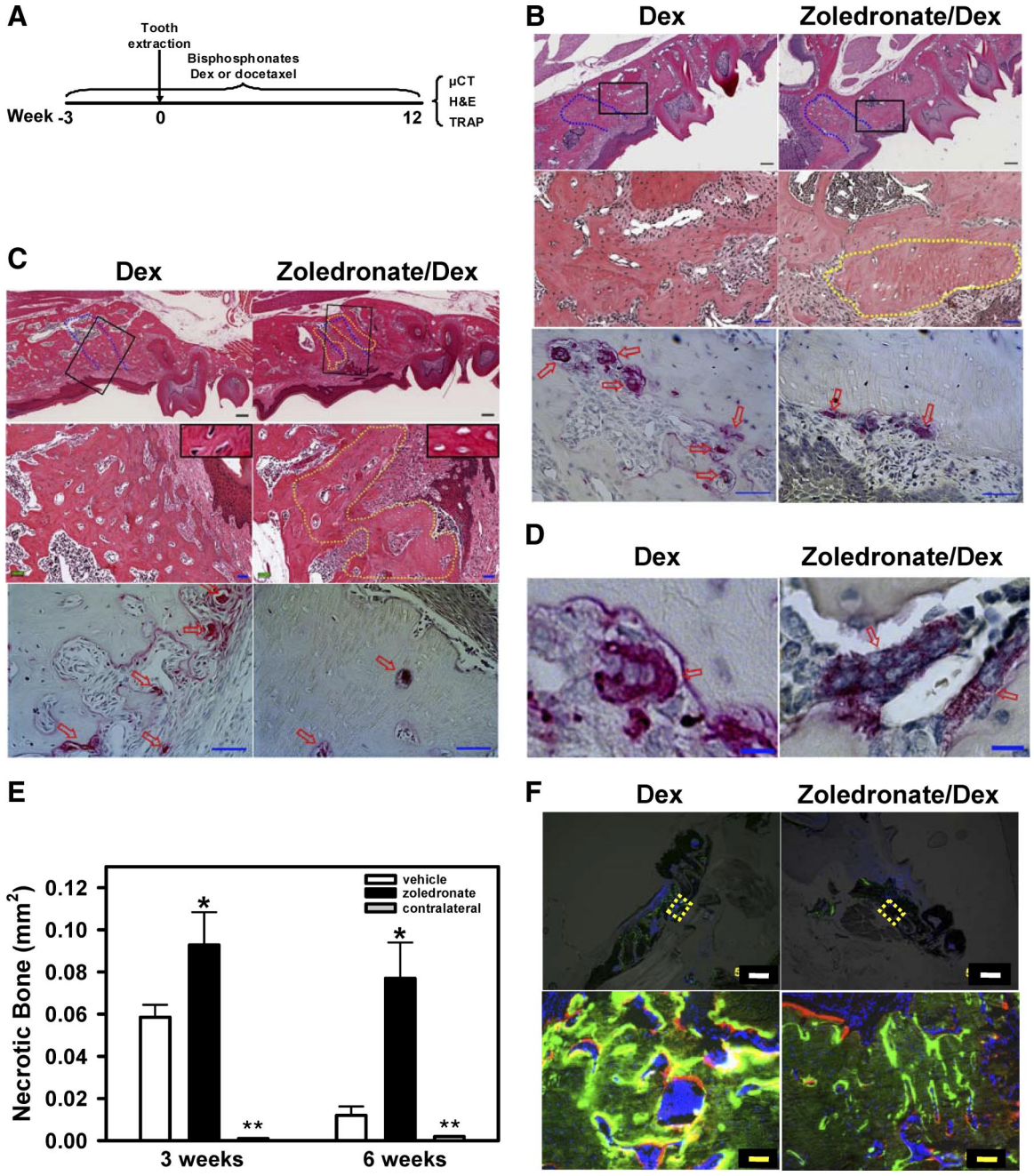

Figure 3. Development of necrotic bone in zoledronate-treated mice following tooth extraction. **A:** Strategy for generating and analyzing zoledronate-induced ONJ-like disease in mice. C57BL6 mice were treated with zoledronate, Dex, docetaxel, or their combinations for three weeks before tooth extraction. The first left maxillary molar tooth was removed and these different drugs were administered for up to 12 weeks. Histological analysis was conducted on the maxilla from Dex-treated (**left panels**) or zoledronate/Dex-treated (**right panels**) mice at three weeks (**B**) and six weeks (**C**) after tooth extraction. **Top panels** show low magnification of H&E staining of the paraffin-embedded sections of the left maxilla (Scale bars = 200 μm). **Blue dotted lines** indicate the extraction socket. **Middle panels** show higher magnification of the areas indicated by the **black squares** in the **top panel** (Scale bars = 50 μm). A **yellow dotted line** circles the dead bone with empty lacunae. **Bottom panels** show the presence of TRAP$^+$ osteoclasts (**red arrows**). Scale bars = 50 μm. **Insets** in the **middle panels** in **C** show lacunae with (**left**) or without (**right**) osteocytes. **D:** TRAP staining of the left maxilla shows the presence of giant osteoclast-like cells in zoledronate/Dex-treated (**right**) but not Dex-treated (**left**) mice three weeks after extraction. Scale bars = 10 μm. **E:** Quantification of the necrotic bone areas in the left or right (contralateral) maxilla of Dex- and zoledronate/Dex-treated mice at three weeks and six weeks after tooth extraction using ImageScope. Data are means ± SEM of three mice. *$P < 0.05$ versus Dex. **Necrotic bone area <0.0005 mm^2. **F:** Dex- and zoledronate/Dex-treated mice were labeled with calcein (green) four weeks and alizarin (red) six weeks after extraction. Higher magnification of the **yellow dotted areas** in the **top panels** (Scale bars = 500 μm) is presented in the corresponding **bottom panels** (Scale bars = 50 μm).

that is commonly used in human cancer patients.[4,14] The selected dosage of dexamethasone (5 mg/kg body weight; weekly) is lower than the equivalent dosage used in cancer patients (~40 mg or 25 mg/m^2).[15] Initially, we tested both intravenous and intraperitoneal routes and found no significant differences (data not shown). Therefore, intraperitoneal injections were used in all experiments.

Given that cumulative exposure to bisphosphonate is a major risk factor for BONJ,[1,8] we maintained mice on high dose of zoledronate or vehicle and examined alveolar bone healing at different time intervals following tooth

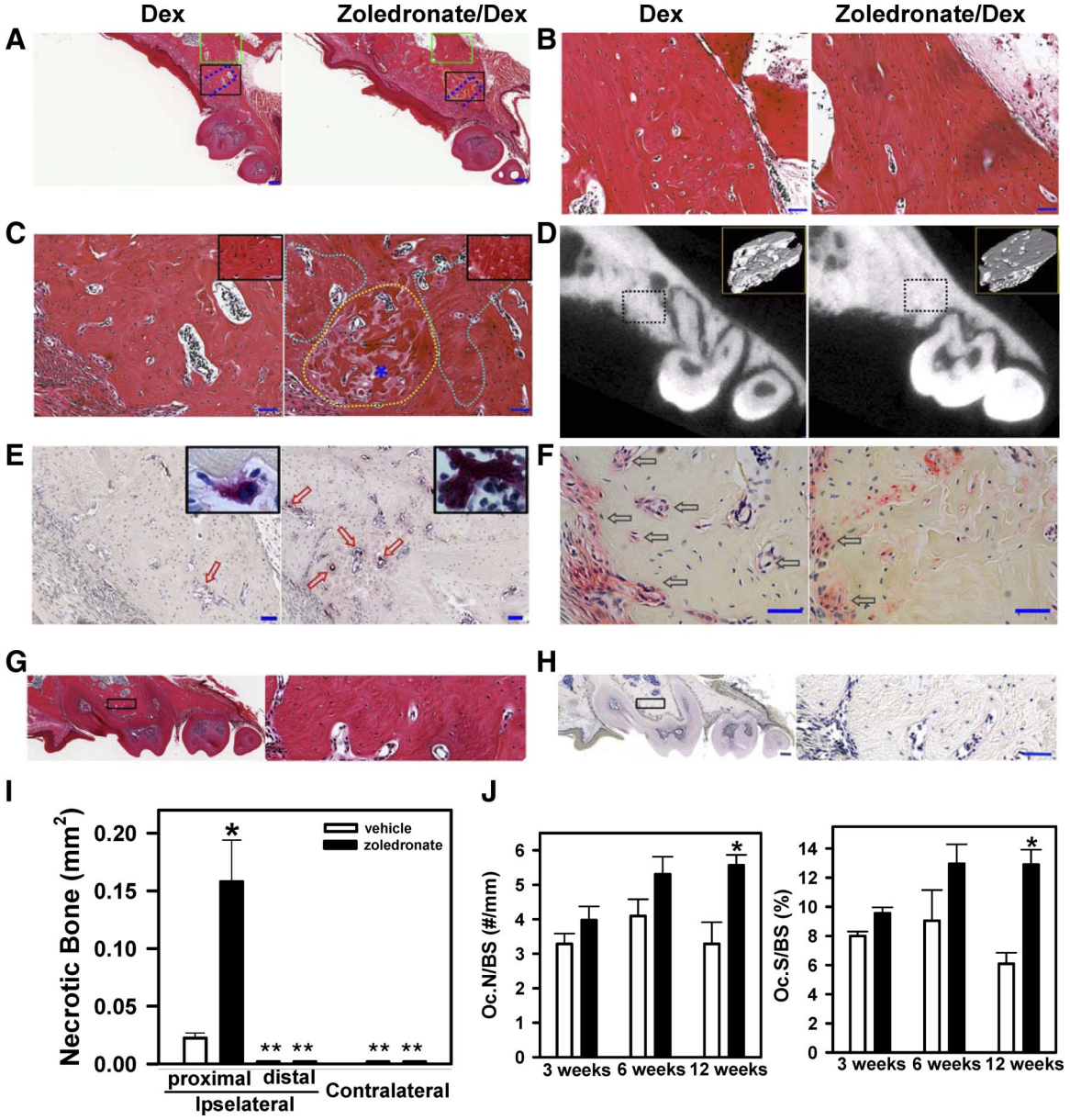

Figure 4. Zoledronate-treated mice develop BONJ-like disease following tooth extraction. **A:** H&E staining of the paraffin-embedded sections of the left maxilla from Dex-treated (**left panels**) or zoledronate/Dex-treated (**right panels**) mice at 12 weeks after tooth extraction. **Blue dotted lines** indicate the extraction socket. **Green squares** and **black squares** indicate the areas distal and proximal to the site of extracted tooth, respectively. **B:** Higher magnification images of the distal areas (**green squares** in **A**) show the presence of viable alveolar bone. **C:** Higher magnification images of the proximal areas (**black squares** in **A**) show the development of BONJ-like disease, characterized by the presence of both sclerotic bone (**yellow dotted line**) and necrotic bone (**white dotted lines**) that were interspersed with viable bone (**right panel**). **Insets** show lacunae with (**left**) or without (**right**) osteocytes. Scale bars for **A–C:** 200 μm. **D:** μCT scan images of the left maxilla illustrates an overall increase in bone density. **Insets** show the three-dimensional reconstructed images of the jaw bone within the region of tooth extraction (**dotted lines**). **E:** TRAP staining (purple; **red arrows**) of the paraffin-embedded sections showed increased osteoclasts in zoledronate-treated mice (**right**). **Insets** show the presence of giant osteoclast-like cell in zoledronate-treated (**right**) but not control (**left**) mice. **F:** ALP staining (red; **black arrows**) of the paraffin-embedded sections shows osteoblasts. Scale bars for **E** and **F:** 50 μm. **G** and **H:** Contralateral maxilla. **Left panels** show low magnification images of H&E-stained (**G**) and TRAP-stained (**H**) paraffin-embedded sections of the right (contralateral) maxilla from zoledronate/Dex-treated mice at 12 weeks after tooth extraction. **Right panels** are the higher magnification of the area in the black square in **left panels**. Scale bars: **left panel**, 200 μm; **right panel**, 50 μm. **I:** Quantification of necrotic bone area in the distal (**B**) and proximal (**C**) regions of the left (ipsilateral) and right (contralateral) maxilla was done by ImageScope. Data are mean ± SEM of seven mice. *$P < 0.05$ versus vehicle. **Necrotic bone area <0.0005 mm^2. **J:** Histomorphometric analysis. The number of osteoclasts per millimeter of bone surface (Oc.N/BS) and the percentage of osteoclast surface per bone surface (Oc.S/BS) were determined (*$P < 0.01$, $n = 3$–6). Open bars: vehicle; filled bars: zoledronate.

extraction (Figure 3A). As shown in Figure 3B, 3 weeks after extraction, the majority of the dead alveolar bone next to the extraction socket was replaced with viable woven bone in Dex-treated mice (Figure 3B; top and middle left panels). In contrast, an increase in necrotic bone with lacunae devoid of osteocytes was observed at the periphery border of the extraction socket in zoledronate-treated mice (Figure 3B, middle right panel; yellow dotted line). Unlike the healing socket of the Dex-treated mice (Figure 3B; bottom left panel), the necrotic zone of the zoledronate-treated mice was largely devoid of $TRAP^+$ osteoclasts (Figure 3B, bottom right panel). Six weeks after injury, the necrotic bones were completely replaced with viable woven and lamellar bone in the extraction sockets of Dex-treated control mice (Figure 3C, top and middle left panels; Figure 3E); however, in zoledronate/Dex-treated mice the necrotic zone remained at the border of the extraction socket (Figure 3C, top and middle right panels, yellow dotted line). The necrotic area of the alveolar bone harbored fewer osteoclasts (Figure 3C, bottom right panel, arrows) compared with the healing socket of control mice (Figure 3C, bottom left panel, arrows). Numerous giant osteoclast-like cells, defined as $TRAP^+$ cells containing 10 or more nuclei (Figure 3D, right panel), were observed within the alveolar bone of the bisphosphonate-treated mice (9.6 ± 1.8% of the total osteoclasts) but very few were present in the Dex-treated control mice (1.7 ± 0.6%; $P = 0.01$, $n = 3$). Finally, two-color fluorescent labeling of the jaw bone demonstrated that zoledronate injection strongly suppressed bone formation at both 4 weeks (green fluorescence) and 6 weeks (red fluorescence) after injury (Figure 3F, bottom right panel) compared with injection of Dex alone.

Long-Term Persistence of the BONJ-Like Disease in Bisphosphonate-Treated Mice

To confirm that bisphosphonate caused defective bone healing rather than just a delay in bone remodeling, we extended our observation beyond the period of 8 weeks, which has been used in clinical diagnosis of BONJ in human patients, following the guidelines established by the American Association of Oral and Maxillofacial Surgeons and American Society for Bone and Mineral Research.[5,16] Twelve weeks after tooth extraction, we found that bone osteonecrosis was present in mice injected with zoledronate/Dex (Figure 4C, right panel), but not Dex alone (Figure 4C, left panel), indicating the development of BONJ-like disease in bisphosphonate-treated mice. In addition to the above criterion, ie, defective bone healing beyond 8 weeks, our diagnosis of BONJ-like disease was also based on the following histological and radiographical criteria: i) the presence of trabeculae of sclerotic lamellar bone with loss of osteocytes from their lacunae (Figure 4C, yellow dotted lines and inset); ii) the presence of irregular trabeculae of pagetoid bone with focal fibrosis that lacked normal bone appearance and matrix structure (Figure 4C, white dotted line); and iii) increased radiopacity of the diseased bone at the injured site as determined by μCT (Figure 4D) that correlates with an increase in bone mineral density (insets: 1120 ± 42 mg/ml for Dex versus 1245 ± 57 mg/ml for zoledronate/Dex) and a decrease in trabecular bone space (Tb. Sp.) (insets: 31.9 ± 9 μm for Dex versus 17.5 ± 1.8 μm for zoledronate/Dex). Active bone necrosis occurred predominantly adjacent to the site of tooth extraction (Figure 4C, right panel), and was not observed at distal sites (Figure 4B) or at the contralateral maxillary sites (Figure 4, G and H). Moreover, bone necrosis was not found in mice injected with Dex alone (Figure 4, A–C, left panels) or without tooth extraction (data not shown). Giant osteoclasts were observed in the alveolar bone of the zoledronate-treated mice (Figure 4E, right panel, inset) but not in control mice (Figure 4E, left panel, inset). Bone histomorphometric analysis demonstrated an increase in osteoclast number (Oc.N/BS; Figure 4J, left panel) and size (Oc.S/BS; Figure 4J, right panel) within the alveolar bone of zoledronate/Dex-treated mice when compared with Dex-treated mice, especially for the 12-week group ($P = 0.009$, $n = 3–6$). The viable lamellar bones taken from the

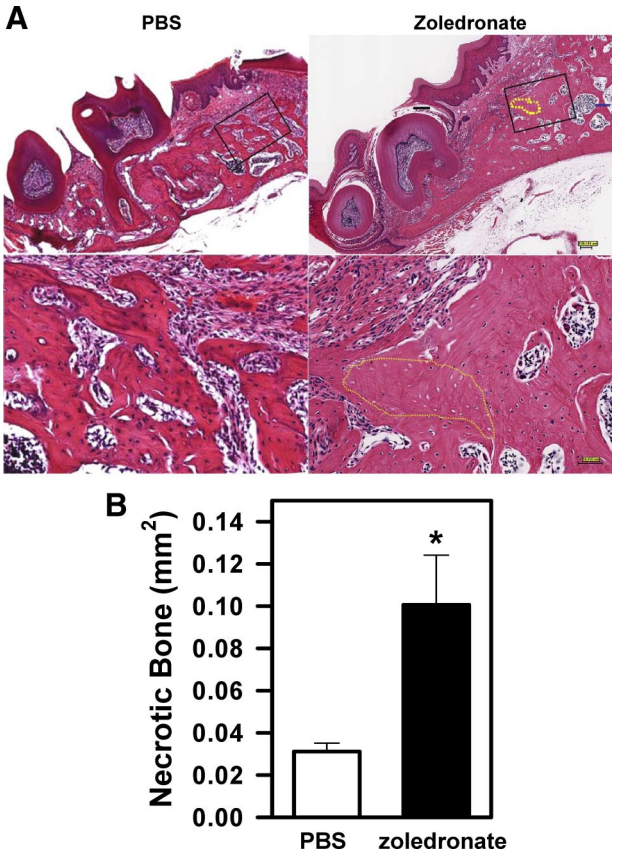

Figure 5. Bisphosphonates are a major cause of BONJ-like disease in mice. **A:** H&E staining of the paraffin-embedded sections of the left maxilla from PBS-treated (**left**) and zoledronate-treated (**right**) mice at 12 weeks after tooth extraction. Lower panels are the higher magnification of the area in the **black square** in the **top panels**. The **yellow dotted lines** indicate areas of necrotic bone. Scale bars: **top panels**, 200 μm; **bottom panels**, 50 μm. **B:** Quantification of the areas of necrotic bone in the left maxilla. Data are means ± SEM of three mice. $^*P < 0.05$ versus PBS.

healing extraction sockets of Dex-treated samples contained a large number of ALP$^+$ osteoblasts (Figure 4F, black arrows), whereas the necrotic region at the extraction socket of zoledronate-treated mice was largely devoid of cell-associated ALP staining (Figure 4F, right panel). Finally, although infection has been suggested as a possible risk factor for BONJ in human patients, we did not observe any clinical signs of infections at the extracted socket of zoledronate-treated mice.

Bisphosphonate Is the Cause of BONJ-Like Disease in Mice

The above experiments showed that bisphosphonates, when injected together with Dex, led to the development of BONJ-like disease in mice. However, it is not known whether bisphosphonates alone would cause BONJ. To address this question, we injected C57BL6 mice with zoledronate or PBS for 3 weeks before and then 12 weeks

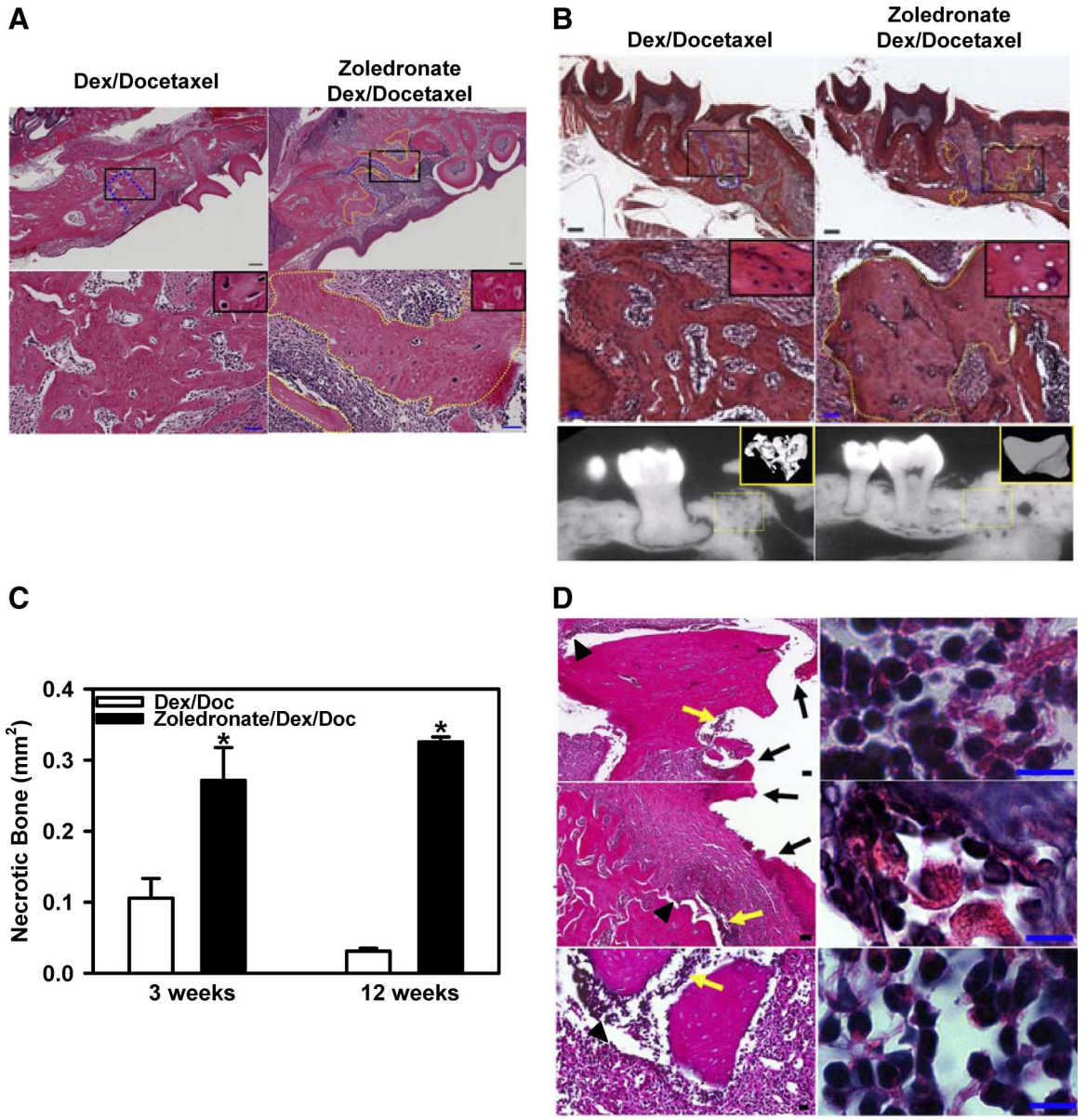

Figure 6. Docetaxel worsens BONJ-like disease in bisphosphonate-treated mice. H&E staining of the paraffin-embedded sections of the left maxilla at three weeks (**A**) and mandible at 12 weeks (**B**) after tooth extraction from Dex/docetaxel-treated (**left panels**) or zoledronate/Dex/docetaxel-treated (**right panels**) mice. **Top panels:** Low magnification of H&E staining of the paraffin-embedded sections of the left maxilla. **Blue dotted lines** indicate the extraction sockets. **Yellow dotted lines** indicate the areas of bone necrosis. **Bottom panels** in **A** and **middle panels** in **B:** Higher magnification of areas in the **black squares** shown in the **top panels**. **Insets** show lacuna with (**left**) or without (**right**) osteocytes. Scale bars: 200 μm (**top panels**) and 50 μm (**bottom panels**). **Bottom panels** in **B:** μCT images of the left maxilla from mice at 12 weeks after tooth extraction. **Insets** showed the three-dimensional reconstructed images of the extraction socket (yellow dotted squares). **C:** Quantification of the areas of necrotic bone in the left maxilla. Data are means ± SEM of 10 mice. $^*P < 0.05$, zoledronate/Dex/docetaxel versus Dex/docetaxel. **D:** Persistent soft tissue defects in mice treated with zoledronate, Dex, and docetaxel at 12 weeks after tooth extraction. Low magnification (**left panels**) of H&E-stained paraffin-embedded sections of the left maxilla shows the disruption of epithelium (**black arrows**), osteomyelitis (**yellow arrows**), and separation of soft tissue from the necrotic bone (**black arrowheads**). High magnification (**right panels**) shows the presence of inflammatory cells within the areas of osteomyelitis. Scale bars: 50 μm (**left panels**) and 10 μm (**right panels**).

after tooth extraction as in Figure 3A. We found that injection of zoledronate but not PBS in mice resulted in the development of BONJ-like disease, as shown by the presence of alveolar bone with empty lacunae (Figure 5A, right panel, yellow dotted lines). The area of dead bone (0.10 mm^2; Figure 5B, filled bar) in zoledronate-treated mice was lower than that observed in zoledronate/Dex-injected mice (0.15 mm^2; Figure 4I). No dead bone was observed in the contralateral jaw (data not shown) or in PBS-injected control mice (Figure 5A, left panels).

Chemotherapy Drugs Worsen BONJ-Like Disease in Bisphosphonate-Treated Mice

Retrospective analyses of human BONJ cases demonstrate a strong correlation among the use of chemotherapy drugs and the development of BONJ. To further verify that our established mouse model of BONJ-like disease does faithfully recapitulate the clinical and histological features of the human disease, we investigated if chemotherapy drugs, such as docetaxel, would worsen BONJ-like disease in bisphosphonate-treated mice. In these experiments, we injected C57BL6 mice intraperitoneally with zoledronate, Dex, and docetaxel based on the regimen in Figure 3A (3 weeks before and 3–12 weeks after tooth extraction). We found that injections of zoledronate, Dex and docetaxel, but not Dex and docetaxel, caused bone death at 3 weeks (Figure 6A, right panels) and 12 weeks (Figure 6B, right panels) following tooth extraction. Histological quantification indicated that mice treated with zoledronate, docetaxel, and Dex developed significantly larger areas of dead bone at both 3 and 12 weeks when compared with mice treated with zoledronate and Dex (0.3 mm^2 in Figure 6C versus 0.15 mm^2 in Figure 4I; $P < 0.05$, $n = 7–11$). At 12 weeks after injury, docetaxel injection also increased the extent and severity of radiopacity of zoledronate/Dex-induced necrotic bone as determined by μCT analysis (3213 mg/ml for three drugs versus 1285 mg/ml for two drugs) (Figure 6B, bottom right panel).

Chemotherapy Drugs Exacerbate Soft Tissue Defects

One of the major clinical criteria for the diagnosis of BONJ in human patients is the presence of soft tissue defects for more than 8 weeks.[5,16] Therefore, we examined whether the BONJ-like disease in our mouse model was also associated with defective soft tissue healing at time points beyond 8 weeks after injury. No soft tissue defect was observed in vehicle-treated mice (Table 1). In the mice treated with bisphosphonates alone, all of them developed osteonecrosis, but none exhibited signs of inflammation or soft tissue disruption. In mice treated with bisphosphonates and Dex, all developed osteonecrosis and a small percentage (3 of 11) of these mice exhibited inflammation and soft tissue defects. In zoledronate/Dex/docetaxel-treated mice, 10 of 10 mice developed osteonecrosis, strong inflammatory response (Figure 6D, left panels, yellow arrows; higher magnification shown in the right panels), bone sequestra (Figure 6D, top and bottom left panels), soft tissue disruption (Figure 6D, left panels, arrowheads), and loss of epithelial coverage (Figure 6D, left panels, black arrows). Close examination of the soft tissue defects revealed several distinct phenotypes, including i) complete disruption of the epithelial layer (Figure 6D, top left panel, black arrows), ii) partial loss of the epithelial coverage (Figure 6D, middle left panel, black arrows), and iii) complete separation of the soft tissue from its underneath necrotic bone (Figure 6D, bottom left panel). All three types of soft tissue defects were associated with the presence of infiltrating leukocytes within the areas of osteomyelitis (Figure 6D, right panels).

Discussion

We report the first mouse model of BONJ-like disease, which elicits major associated risk factors identified in the human disease, including its dependence on long-term use of bisphosphonates, immunosuppressive and chemotherapy drugs, and mechanical trauma. We show that the BONJ-like disease developed in mice exhibits the characteristic human disease of osseous sclerosis, sequestra, avascular, and radiopaque alveolar bone in the jaw, as well as impaired epithelial coverage, as demonstrated by computed tomography and histological studies. In addition, we show that administration of bisphosphonates in mice led to an increase in osteoclast number and size within the alveolar jaw bone and the formation of giant osteoclast-like cells. Most importantly, we demonstrate that the BONJ-like disease developed in bisphosphonate-treated mice exhibited the hallmark of BONJ in human patients, including the persistent presence of bone sclerosis and soft tissue defects at the surgical site.

Table 1. Soft Tissue Defects in Bisphosphonate-treated Mice

	Vehicle; no. affected (total)	Zoledronate; affected (total)	Zoledronate/Dex; affected (total)	Zoledronate/Dex/docetaxel; affected (total)
Necrotic bone	0 (9)	3 (3)	11 (11)	10 (10)
Inflammation	0 (9)	0 (3)	3 (11)	10 (10)
Soft tissue defects	0 (9)	0 (3)	3 (11)	10 (10)

Mice were injected twice weekly with different combinations of zoledronate, Dex, and docetaxel, or vehicle (PBS, Dex, or Dex/docetaxel) for 3 weeks before and then 12 weeks after tooth extraction. The number of mice that exhibited bone necrosis, inflammation, and soft tissue defects, and the total number of mice examined are summarized.

Several risk factors have been identified based on clinical studies for the development of BONJ in cancer patients on bisphosphonate therapy.[1–5] These include long-term use of high dose aminobisphosphonates, in conjunction with other co-morbid conditions such as dental surgery (eg, tooth extraction), oral trauma, and poor dental hygiene.[4] In addition, BONJ strongly correlates with the use of chemotherapy drugs (eg, docetaxel) and immunosuppressive agents (eg, corticosteroids). A major obstacle in elucidating the pathophysiology of this disease is the simultaneous use of multiple therapeutic drugs in cancer patients, which are required to control both tumor growth and its related skeletal complications.[6,17] Thus, animal models are urgently needed to decipher the underlying pathogenesis of BONJ leading to better diagnosis, prediction of disease susceptibility, prevention, and treatment. The availability of this mouse model will allow accurate delineation of the pathology of the disease at the cellular and biochemical levels, leading to future development of new clinical and laboratory endpoints for accurate diagnosis and prediction of BONJ in humans.

Our study demonstrates that bisphosphonates, but not immunosuppressive or chemotherapy drugs, are the major cause of BONJ. We show that simultaneous administration of chemotherapy drugs increases the severity of the disease, especially the incidence of soft tissue defects. Our observations agree well with clinical observations that the majority of BONJ cases are associated with the high-risk cancer patients.[1–5] The abilities of anti-neoplastic drugs to accelerate BONJ is likely attributed to their ability to block endothelia cell migration and proliferation[18,19] as well as bone repair/regeneration. It should also be emphasized that our current study focused primarily on intraperitoneal/intravenous administration of high dose zoledronate that is commonly used in cancer patients.[4,14] Whether low dosages or other routes of administration of bisphosphonates also cause BONJ is unclear. The availability of this mouse model should allow us to address all of these important questions experimentally in the near future.

Bisphosphonates function to stabilize bone mineral density in cancer patients primarily by inhibiting osteoclast-mediated bone resorption. Though bisphosphonates can induce osteoclast apoptosis *in vitro*,[20] their impact on osteoclast number and size as well as on osteoblast-mediated bone formation *in vivo* remains controversial.[21–25] We found that short-term administration (1 week following tooth extraction; no pretreatment) of bisphosphonates in mice reduced the number of both osteoclasts and osteoblasts within the extraction socket (Figure 2, C and E, right panels), likely due to the suppression of osseous angiogenesis induced by zoledronate (Figure 2B, right panel). Surprisingly, long-term bisphosphonate treatment (3 weeks before plus 12 weeks after tooth extraction) led to significantly increased number and size of osteoclasts within the alveolar bone (Figure 4J). In addition, we found that administration of bisphosphonates resulted in the formation of giant osteoclast-like cells, which were often detached from the alveolar bone surface (Figure 3D, right panel). In a strong support of these novel observations in mice, it was recently reported that long-term injection of nitrogen-containing bisphosphonates in human patients resulted in a similar increase in the number and size of osteoclasts, as well as in the formation of giant osteoclasts *in vivo*.[23]

Mechanistically, we show that i) mechanical injury led to an early phase of bone death, which requires a minimum of 3 weeks to repair naturally in the absence of bisphosphonates; ii) administration of bisphosphonates suppressed angiogenesis and bone remodeling within the alveolar bone, which led to the accumulation of necrotic bone at the site of injury; and iii) administration of chemotherapy drugs further exacerbates BONJ-like disease in bisphosphonate-treated mice, resulting in a variety of soft tissue defects, which persisted beyond 12 weeks following tooth injury. In this regard, a rat model of BONJ-like recently reported by Sonis et al.[26] failed to meet the requirement of non-healing soft tissue beyond 8 weeks after injury. In their study, the investigators extracted all three molars, which caused significant soft tissue destruction. They reported that mucosal ulceration developed in majority of the zoledronate/dexamethasone-treated rats at 14 days and 28 days after tooth extraction, when compared with control rats. In light of our observations that natural bone repair/regeneration in mice took a minimum of 21 days to complete, it is likely that a similar time period or longer would be required for the natural bone healing process to complete in rats as well. Thus, whether the higher incidence (80–100%) of mucosal ulceration observed in the rat model reflects a delay in wound healing in the presence of zoledronate and dexamethasone, or supports the development of BONJ-like disease in rats, remains to be determined.

In conclusion, using a clinically relevant setting, we find that administration of zoledronate, dexamethasone, and docetaxel leads to bone necrosis and intense inflammation within the extracted alveolar socket well beyond the period of natural wound healing, which in combination causes the detachment of the epithelium from its underneath jaw bone. The defective alveolar bone repair and the presence of soft tissue defects beyond 12 weeks after tooth injury in our mouse model are in line with the defined clinical criteria for the diagnosis of human BONJ. Thus, the availability of this novel mouse model of BONJ-like disease not only provides us with the opportunity to conduct prospective and well-controlled studies to evaluate different risk factors in the etiology of BONJ, it could also be used to develop new therapeutic strategies to prevent and cure this debilitating disease in human patients.

Acknowledgments

We thank Dr. George Huang for technical advice and Dr. Alfredo A. Molinolo and Elizabeth P. Smith for help with histology.

References

1. Bamias A, Kastritis E, Bamia C, Moulopoulos LA, Melakopoulos I, Bozas G, Koutsoukou V, Gika D, Anagnostopoulos A, Papadimitriou

C, Terpos E, Dimopoulos MA: Osteonecrosis of the jaw in cancer after treatment with bisphosphonates: incidence and risk factors. J Clin Oncol 2005, 23:8580–8587
2. Ruggiero SL, Woo SB: Bisphosphonate-related osteonecrosis of the jaws. Dent Clin North Am 2008, 52:111–128
3. Kuehn BM: Reports of adverse events from bone drugs prompt caution. JAMA 2006, 295:2833–2836
4. Woo SB, Hellstein JW, Kalmar JR: Systematic review: bisphosphonates and osteonecrosis of the jaws. Ann Intern Med 2006, 144:753–761
5. Khosla S, Burr D, Cauley J, Dempster DW, Ebeling PR, Felsenberg D, Gagel RF, Gilsanz V, Guise T, Koka S, McCauley LK, McGowan J, McKee MD, Mohla S, Pendrys DG, Raisz LG, Ruggiero SL, Shafer DM, Shum L, Silverman SL, Van Poznak CH, Watts N, Woo SB, Shane E: Bisphosphonate-associated osteonecrosis of the jaw: report of a task force of the American Society for Bone and Mineral Research. J Bone Miner Res 2007, 22:1479–1491
6. Wang J, Goodger NM, Pogrel MA: Osteonecrosis of the jaws associated with cancer chemotherapy. J Oral Maxillofac Surg 2003, 61:1104–1107
7. Marx RE: Pamidronate (Aredia) and zoledronate (Zometa) induced avascular necrosis of the jaws: a growing epidemic. J Oral Maxillofac Surg 2003, 61:1115–1117
8. Durie BG, Katz M, Crowley J: Osteonecrosis of the jaw and bisphosphonates. N Engl J Med 2005, 353:99–102
9. Hansen T, Kunkel M, Weber A, James KC: Osteonecrosis of the jaws in patients treated with bisphosphonates: histomorphologic analysis in comparison with infected osteoradionecrosis. J Oral Pathol Med 2006, 35:155–160
10. Bi Y, Ehirchiou D, Kilts TM, Inkson CA, Embree MC, Sonoyama W, Li L, Leet AI, Seo BM, Zhang L, Shi S, Young MF: Identification of tendon stem/progenitor cells and the role of the extracellular matrix in their niche. Nat Med 2007, 13:1219–1227
11. Miao D, Scutt A: Histochemical localization of alkaline phosphatase activity in decalcified bone and cartilage. J Histochem Cytochem 2002, 50:333–340
12. Parfitt AM, Drezner MK, Glorieux FH, Kanis JA, Malluche H, Meunier PJ, Ott SM, Recker RR: Bone histomorphometry: standardization of nomenclature, symbols, and units. Report of the ASBMR Histomorphometry Nomenclature Committee. J Bone Miner Res 1987, 2:595–610
13. Bovetti S, Hsieh YC, Bovolin P, Perroteau I, Kazunori T, Puche AC: Blood vessels form a scaffold for neuroblast migration in the adult olfactory bulb. J Neurosci 2007, 27:5976–5980
14. Reid IR, Brown JP, Burckhardt P, Horowitz Z, Richardson P, Trechsel U, Widmer A, Devogelaer JP, Kaufman JM, Jaeger P, Body JJ, Brandi ML, Broell J, Di Micco R, Genazzani AR, Felsenberg D, Happ J, Hooper MJ, Ittner J, Leb G, Mallmin H, Murray T, Ortolani S, Rubinacci A, Saaf M, Samsioe G, Verbruggen L, Meunier PJ: Intravenous zoledronic acid in postmenopausal women with low bone mineral density. N Engl J Med 2002, 346:653–661
15. Richardson PG, Sonneveld P, Schuster MW, Irwin D, Stadtmauer EA, Facon T, Harousseau JL, Ben Yehuda D, Lonial S, Goldschmidt H, Reece D, San Miguel JF, Blade J, Boccadoro M, Cavenagh J, Dalton WS, Boral AL, Esseltine DL, Porter JB, Schenkein D, Anderson KC: Bortezomib or high-dose dexamethasone for relapsed multiple myeloma. N Engl J Med 2005, 352:2487–2498
16. American Association of Oral and Maxillofacial Surgeons position paper on bisphosphonate-related osteonecrosis of the jaws. J Oral Maxillofac Surg 2007, 65:369–376
17. Dunstan CR, Felsenberg D, Seibel MJ: Therapy insight: the risks and benefits of bisphosphonates for the treatment of tumor-induced bone disease. Nat Clin Pract Oncol 2007, 4:42–55
18. Lyseng-Williamson KA, Fenton C: Docetaxel: a review of its use in metastatic breast cancer. Drugs 2005, 65:2513–2531
19. Grant DS, Williams TL, Zahaczewsky M, Dicker AP: Comparison of antiangiogenic activities using paclitaxel (Taxol) and docetaxel (Taxotere). Int J Cancer 2003, 104:121–129
20. Reszka AA, Halasy-Nagy JM, Masarachia PJ, Rodan GA: Bisphosphonates act directly on the osteoclast to induce caspase cleavage of mst1 kinase during apoptosis: a link between inhibition of the mevalonate pathway and regulation of an apoptosis-promoting kinase. J Biol Chem 1999, 274:34967–34973
21. Hughes DE, Wright KR, Uy HL, Sasaki A, Yoneda T, Roodman GD, Mundy GR, Boyce BF: Bisphosphonates promote apoptosis in murine osteoclasts in vitro and in vivo. J Bone Miner Res 1995, 10:1478–1487
22. Fisher JE, Rodan GA, Reszka AA: In vivo effects of bisphosphonates on the osteoclast mevalonate pathway. Endocrinology 2000, 141:4793–4796
23. Weinstein RS, Roberson PK, Manolagas SC: Giant osteoclast formation and long-term oral bisphosphonate therapy. N Engl J Med 2009, 360:53–62
24. von Knoch F, Jaquiery C, Kowalsky M, Schaeren S, Alabre C, Martin I, Rubash HE, Shanbhag AS: Effects of bisphosphonates on proliferation and osteoblast differentiation of human bone marrow stromal cells. Biomaterials 2005, 26:6941–6949
25. Idris AI, Rojas J, Greig IR, Van't Hof RJ, Ralston SH: Aminobisphosphonates cause osteoblast apoptosis and inhibit bone nodule formation in vitro. Calcif Tissue Int 2008, 82:191–201
26. Sonis ST, Watkins BA, Lyng GD, Lerman MA, Anderson KC: Bony changes in the jaws of rats treated with zoledronic acid and dexamethasone before dental extractions mimic bisphosphonate-related osteonecrosis in cancer patients. Oral Oncol 2009, 45:164–172